Liquid Crystals
Publication details, including instructions for authors and subscription information:
http://www.informaworld.com/smpp/title~content=t713926090

Synthesis and mesomorphic properties of resorcyl di[4-(4-alkoxy-2,3-diflorophenyl)ethynyl] benzoate liquid crystals

Ziming Li[a]; Peter Salamon[b]; Antal Jakli[b]; Kan Wang[c]; Chuan Qin[a]; Qing Yang[d]; Cheng Liu[d]; Jianxun Wen[d]
[a] School of Chemistry and Molecular Engineering, East China University of Science and Technology, Meilong Road 130, Shanghai, PR China [b] Liquid Crystal Institute, Kent State University, Kent, OH, USA [c] University of Pittsburgh, Pittsburgh, PA, USA [d] Shanghai Tianwen Chemical Corporation, Xitai Road 237, Shanghai, PR China

Online publication date: 23 April 2010

To cite this Article Li, Ziming , Salamon, Peter , Jakli, Antal , Wang, Kan , Qin, Chuan , Yang, Qing , Liu, Cheng and Wen, Jianxun(2010) 'Synthesis and mesomorphic properties of resorcyl di[4-(4-alkoxy-2,3-diflorophenyl)ethynyl] benzoate liquid crystals', Liquid Crystals, 37: 4, 427 — 433
To link to this Article: DOI: 10.1080/02678291003632652
URL: http://dx.doi.org/10.1080/02678291003632652

Liquid Crystals,
Vol. 37, No. 4, April 2010, 427–433

Taylor & Francis
Taylor & Francis Group

Synthesis and mesomorphic properties of resorcyl di[4-(4-alkoxy-2,3-diflorophenyl)ethynyl] benzoate liquid crystals

Ziming Li[a], Peter Salamon[b], Antal Jakli[b], Kan Wang[c], Chuan Qin[a]*, Qing Yang[d], Cheng Liu[d] and Jianxun Wen[d]

[a]*School of Chemistry and Molecular Engineering, East China University of Science and Technology, Meilong Road 130, Shanghai 200237, PR China;* [b]*Liquid Crystal Institute, Kent State University, Kent, OH 44242, USA;* [c]*University of Pittsburgh, Pittsburgh, PA 15213, USA;* [d]*Shanghai Tianwen Chemical Corporation, Xitai Road 237, Shanghai 200232, PR China*

(Received 1 October 2009; final version received 18 January 2010)

Two resorcyl di[4-(4-alkoxy-2,3-difluorophenyl)ethynyl] benzoate liquid crystals (**A10** and **A12**) were prepared and their mesomorphic properties were observed. A large polarisation value was obtained with longer terminal chains.

Keywords: liquid crystals; spontaneous polarisation; banana-shaped; fluorinated

1. Introduction

In the mid 1990s a novel type of mesogenic material brought new expectations for liquid crystal research: the so-called banana-shaped liquid crystal or bent-core liquid crystal. Today, this sort of material is an active field of research in both mesogenic materials for application and basic supramolecular science (for a recent review about bent-core mesogens see [1]). In the last decade extensive research has been carried out on bent-core liquid crystals [2, 3] and the results have revealed a great variety of novel chemical and physical properties. Many novel and intriguing mesophases were observed, in particular the induction of supramolecular chirality using achiral molecules and the noticeable optical, ferroelectric and antiferroelectric properties of these materials [4]. In bent-core materials the macroscopic polarisation values are often greater than 500 nC cm^{-2}, which could be useful for non-linear optical applications. In addition, their antiferroelectric and ferroelectric [5] and flexoelectric [6] properties may also be useful in display and electromechanical applications [7].

In the last decade, considerable improvement occurred in the synthesis of fluoro-substituted bent-core liquid crystal materials [8–13]. Fluoro-substitution brings unique properties not only to rod-shape mesogens [14, 15], but also to bent-core liquid crystals; for example, we reported achiral antiferroelectric bent-core liquid crystals (**A*n***, $n = 4$ and 8, Figure 1) containing a 2,3-difluorotolane unit, at a time when no liquid crystal phase was observed for compounds without fluoro-substituents [16]. However, the polarisation was found to be small (when $n = 8$, 130 nC cm^{-2}), which may be less desirable for applications [16]. In order to obtain better mesomorphic properties, two new compounds with longer terminal chains ($n = 10$ and 12) have been prepared and their mesomorphic properties measured. The result indicates that a much larger ($P > 800$ nC cm^{-2}) polarisation value can be obtained.

2. Experimental

All compounds were prepared following the synthetic pathway shown in Scheme 1.

2.1 Ethyl 4-[(4-n-decoxy-2,3-difluorophenyl) ethynyl]-benzoate (2a)

Compound **1a** (1.77 g, 6.0 mmol), ethyl-4-iodo-benzoate (1.6 g, 6.0 mmol), bis(triph-enylphosphine)-palladiumdichloride (0.09 g), copper (I) iodide (0.10 g), triphenylphosphine (0.16 g) and anhydrous triethylamine (25 mL) were placed in a 50 mL flask; the mixture was stirred at 60°C for 5 h under nitrogen. After the reaction was completed, the precipitation was filtered off and washed with toluene (50 mL). The filtrate was washed with water, and dried over anhydrous magnesium sulphate. The solvent was removed *in vacuo* and the residue was purified by column chromatography on silica gel using petroleum ether (b.p. 60–90°C)/ethyl acetate (20/1) as the eluent. Removal of the solvent from the eluate gave 1.30 g (94%) of the title product (**2a**) as a white solid.

MS (m/z, %): 442 (M^+, 23), 274 (100); ^{1}H NMR ($CDCl_3$, 500 MHz), δ (ppm): 0.89 (t, 3H, CH_3, $J = 6.8$ Hz), 1.2–1.4 (m, 12H), 1.41 (t, 3H, $COOCH_2CH_3$, $J = 7.6$ Hz), 1.47 (m, 2H, $ArOCH_2$ CH_2CH_2-), 1.83 (m, 2H, $ArOCH_2CH_2$-), 4.07 (t, 2H, $ArOCH_2$-, $J = 6.6$ Hz), 4.39 (m, 2H, $COOCH_2$-), 6.72 (t, 1H, Ar-H, $J = 8.1$ Hz), 7.20 (m, 1H, Ar-H), 7.59 (d, 2H, Ar-H, $J = 8.3$ Hz), 8.03 (d, 2H, Ar-H, $J = 8.3$ Hz).

*Corresponding author. Email: qinchuan@ecust.edu.cn

ISSN 0267-8292 print/ISSN 1366-5855 online

DOI: 10.1080/02678291003632652
http://www.informaworld.com

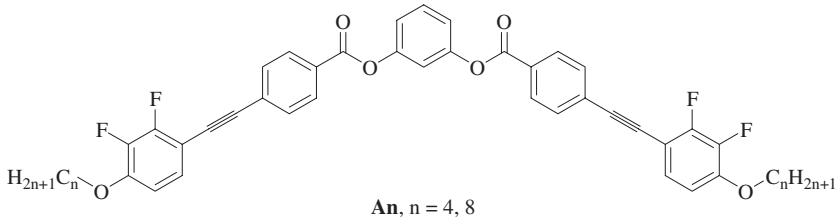

An, n = 4, 8

Figure 1. 2,3-difluorotolane achiral bent-core liquid crystals showing an antiferroelectric smectic phase.

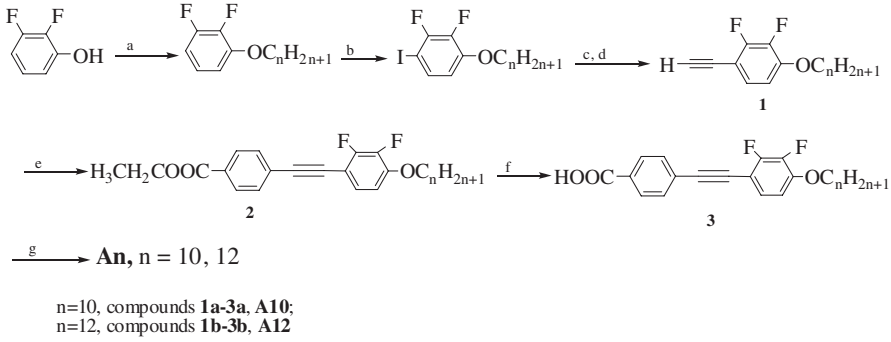

Scheme 1. Synthetic pathway used to prepare the bent-core liquid crystal compounds **A*n*.** Reagents and conditions: (a) $H(CH_2)_nBr$, K_2CO_3, DMF, 120°C; (b) *n*-BuLi, –78°C, then I_2/THF; (c) 2-methyl-3-butyn-2-ol, $Pd(PPh_3)_2Cl_2$, CuI,Et_3N; (d) KOH, toluene; (e) methyl-4-iodobenzoate, $Pd(PPh_3)_2Cl_2$, CuI,Et_3N; (f) NaOH, MeOH, H_2O; (g) *m*-diphenol, DCC, cat.DMAP, THF.

*2.2 Ethyl 4-[(4-*n*-dodecoxy-2,3-difluorophenyl) ethynyl]-benzoate (2b)*

Compound **2b** was prepared using a procedure similar to that described for the synthesis of **2a**.

MS (m/z, %): 470 (M^+, 9), 302 (100); ^{1}H NMR ($CDCl_3$, 500 MHz), δ (ppm): 0.90 (t, 3H, CH_3, $J = 6.8$ Hz), 1.2–1.5 (m, 21H), 1.80 (m, 2H, $ArOCH_2CH_2$-), 4.05 (t, 2H, $ArOCH_2$-, J = 6.5 Hz), 4.39 (m, 2H, $COOCH_2$-), 6.72 (m, 1H, Ar-H), 7.19 (m, 1H, Ar-H), 7.60 (d, 2H, Ar-H, J = 8.3 Hz), 8.07 (d, 2H, Ar-H, J = 8.3 Hz).

*2.3 4-[(4-*n*-decoxy-2,3-difluoro phenyl)ethynyl] benzoic acid (3a)*

Sodium hydroxide(0.48 g, 12 mmol) was added to a mixture of **2a** (1.29 g, 2.92 mmol), CH_3OH (30 mL), H_2O (10 mL). The mixture was stirred at room temperature and monitored by thin layer chromotography (TLC) until the starting materials had disappeared. Then HCl (10%) was added slowly to reach a pH = 3. The precipitate was filtered and washed with water. The solid was recrystallised from ethanol to yield 1.01 g (83.5%) of the title compound as a white crystal.

MS (m/z, %): 414 (M^+, 14), 274 (100); ^{1}H NMR-($CDCl_3$, 500 MHz), δ (ppm): 0.87 (t, 3H, CH_3, $J = 6.8$ Hz), 1.2–1.4 (m, 12H), 1.49 (m, 2H, $ArOCH_2CH_2CH_2$-), 1.83 (m, 2H, $ArOCH_2CH_2$-), 4.19 (t, 2H, $ArOCH_2$-, J = 6.5 Hz), 7.06 (m, 1H, Ar-H), 7.38(m, 1H, Ar-H), 7.68 (d, 2H, Ar-H, J = 8.3 Hz,), 8.07 (d, 2H, Ar-H, J = 8.3 Hz).

*2.4 4-[(4-*n*-dodecoxy-2,3-difluoro phenyl)ethynyl] benzoic acid (3b)*

Compound **3b** was prepared using a procedure similar to that described for the synthesis of **3a**.

MS (m/z, %): 442 (M^+, 15), 274 (100); ^{1}H NMR ($CDCl_3$, 500 MHz), δ (ppm): 0.90 (t, 3H, CH_3, $J = 6.8$ Hz), 1.2–1.5 (m, 18H), 1.81 (m, 2H, $ArOCH_2CH_2$-), 4.07 (t, 2H, $ArOCH_2$-, $J = 6.5$ Hz), 6.71 (m, 1H, Ar-H), 7.19 (m, 1H, Ar-H), 7.62 (d, 2H, Ar-H, $J = 8.3$ Hz), 8.07 (d, 2H, Ar-H, $J = 8.3$ Hz).

*2.5 Resorcyl di[4-(4-*n*-decoxy-2,3-difluorophenyl)-ethynyl] benzoate (A10)*

A mixture of compound **3a** (0.58 g, 1.4 mmol), *m*-phendiol (0.07 g, 0.636 mmol), a catalytic amount of 4-(N,N-dimethyl-amino)pyridine (DMAP, 0.01 g, 0.082 mmol) and dry tetrahydrofuran (THF) (10 mL) was stirred at room temperature for 10 min. To this solution, N,N'-dicyclohexylcarbodiimide (DCC, 0.07 g, 0.636 mmol) was added and stirred for 48 h. The precipitated N,N'-

dicyclohexylurea was filtered off and washed with dichloro-methane (25 mL). The filtrate was washed successively with 5% aqueous acetic acid (25 mL), 5% ice-cold sodium hydroxide solution (2 × 25 mL), water (3 × 25 mL) and dried over anhydrous sodium sulphate. The solvent was removed to yield a residue which was purified by column chromatography on silica gel using chloroform/petroleum ether (20/14) as eluent. The solvent was removed *in vacuo* and a white material was produced. After recrystallisation from a mixture of acetone/methanol, 0.22 g (41%) of the title compound was produced as a white crystal.

MS (m/z, %): 902 (M^+, 0.17), 397 (100); ^{1}H NMR ($CDCl_3$, 500 MHz), δ (ppm): 0.89 (t, 6H, $2CH_3$, $J = 6.9$ Hz), 1.2–1.4 (m, 24H), 1.47 (m, 4H, $2ArOCH_2CH_2CH_2$-), 1.84 (m, 4H, $2ArOCH_2CH_2$-), 4.08 (t, 4H, $2ArOCH_2$-, $J = 6.6$ Hz), 6.73 (t, 2H, Ar-H, $J = 7.5$ Hz), 7.10–7.30 (m, 5H, Ar-H), 7.50 (m, 1H, Ar-H), 7.67 (d, 4H, Ar-H, $J = 8.4$ Hz), 8.18 (d, 4H, Ar-H, $J = 8.4$ Hz); IR (KBr, ν_{max}, cm^{-1}): 2957, 2920, 2852, 2214, 1737, 1603, 1516, 1472, 1302, 1128, 1082, 1018, 891, 852, 802, 763, 688.

2.6 *Resorcyl di[4-(4-n-dodecoxy-2,3-difluorophenyl)-ethynyl] benzoate (A12)*

Compound **A12** was prepared using a procedure similar to that described for the synthesis of **A10**.

MS (m/z, %): 958 (M^+, 15), 425 (100); ^{1}H NMR ($CDCl_3$, 500 MHz), δ (ppm): 0.88 (t, 6H, $2CH_3$, $J = 6.8$ Hz), 1.20–1.40 (m, 32H), 1.47 (m, 4H, $2ArOCH_2CH_2$ C H_2-), 1.84 (m, 4H, $2ArOCH_2CH_2$-), 4.07 (t, 4H, $2ArOCH_2$-, $J = 6.6$ Hz), 6.73 (t, 2H, Ar-H, $J = 7.9$ Hz), 7.10–7.30 (m, 5H, Ar–H), 7.50 (m, 1H, Ar-H), 7.67 (d, 4H, Ar-H, $J = 8.3$ Hz), 8.18 (d, 4H, Ar-H, $J = 8.2$ Hz); IR (KBr, ν_{max}, cm^{-1}): 2954, 2917, 2850, 1732, 1601, 1520, 1474, 1303, 1303, 1278, 1138, 1086, 1016, 889, 855, 804, 760, 689.

3. Mesophase properties

3.1 *Experimental techniques*

The dielectric studies were carried out using a Schlumberger 1260 impedance/gain-phase analyser at 10 kHz frequency using a 0.1 V (RMS) measurement voltage. For the impedance measurements, a four-wired configuration was used in order to eliminate the distortive contribution of the connecting wires. For the sake of precision, the instrument was calibrated with a 1 kΩ resistor. The dielectric measurements were analysed according to a procedure described elsewhere [17].

The dielectric properties of the substances were investigated in laboratory-made 5 μm thick sandwich cells with inner Indium Tin Oxides (ITO) coating that served as the electrodes.

For the polarisation current, transmission and textural measurements, 5 μm thick, 0.25 mm^2 electrode area cells with rubbed polyimide coated surfaces (supplied by E.H.C. Co. Ltd., Japan) were used. Optical transmission measurements were performed on all materials with an Olympus BX60 polarising microscope fitted with a custom-made heating stage and photodiode with a rubbing direction at 45° to the crossed analyser and polariser. For the polarisation current measurements, triangular voltage signals were applied by a HP33120A function generator and an FLC F20AD voltage amplifier, and the time dependence of the current signal was measured using a picoscope.

3.2 *Results*

3.1.1 *Compound A10*

The temperature dependence of the transmitted light intensity is plotted in Figure 2. It can be seen that with heating, the crystalline state melts almost directly to the isotropic phase (with only about a 0.3°C mesophase range), but with cooling it has a mesophase from 127°C to 119°C.

The temperature dependence of the dielectric constant measured at 10 kHz is shown in Figure 3. The large dielectric constant in the mesophase range indicates a polar (ferroelectric or partially antiferroelectric) structure [18].

The time dependencies of the polarisation currents at different temperatures are shown in Figure 5(a). One can see that the material is mainly antiferroelectric with a polarisation value reaching as high as 850 nC cm^{-2} at 124°C. The temperature dependence of the magnitude of the polarisation is plotted in Figure 5(b).

The time dependence of the polarisation current under square-wave electric fields reveals a fast switching without time delay, with switching times ranging from 27 μs to 43 μs for applied fields ranging from 7 V/μm to 2 V/μm at 126°C. The gradual change of the polarisation current curves under extended

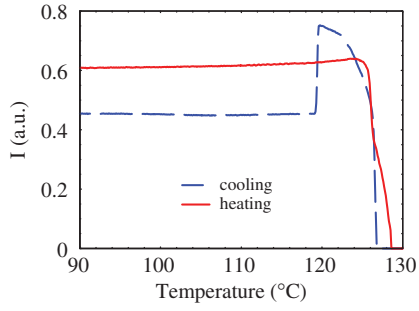

Figure 2. Temperature dependence of the transmitted light intensity measured in 5 μm thick film of **A10** for cooling and heating with 1°C/min cooling/heating rates.

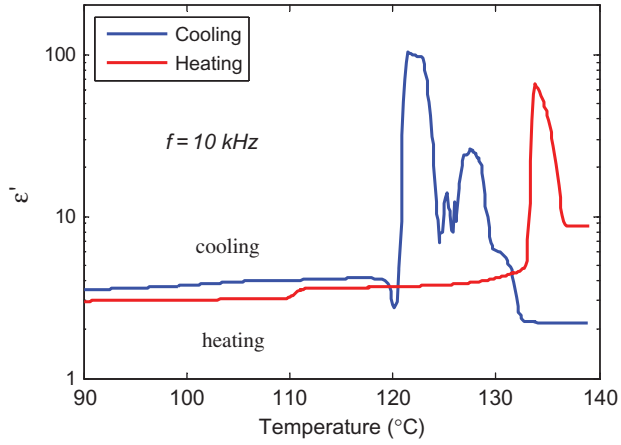

Figure 3. Temperature dependence of the dielectric constant measured at 10 kHz in **A10**.

application of square-wave electric fields shows a gradual change of the threshold switching voltage after the electric field is applied as shown in Figure 6. This gradual change most probably is due to gradually turning the originally oblique layers to an upright position.

After the layers are transformed to the upright position, the textures show the typical antiferroelectric racemic (SmC_sPA) phase: the initial state has a stripe texture (see Figure 4(c)), and when they are transferred to the ferroelectric phase the texture is smooth with rotation of the optic axis upon sign reversal of the applied square-wave field (see Figure 4(d)). Here we note that this switching behaviour is very similar to that which we observed earlier on another material [19].

3.2.2 *Compound A12*

The temperature dependence of the transmitted light intensity in **A12** is plotted in Figure 7. It shows a very similar phase sequence to **A10**. With heating, the crystalline state melts directly to the isotropic phase, but with cooling it has a mesophase from 127°C to 120°C.

The temperature dependence of the dielectric constant measured at 10 kHz is shown in Figure 8. Similar to **A10,** the mesophase is polar (antiferroelectric or partially ferroelectric).

The time dependence of the polarisation current in Figure 9 shows partially antiferroelectric and ferroelectric responses at 23 Hz. It also shows the alignment effect of the electric field in time.

From the time integral of the polarisation peak we deduce that the maximum value of the polarisation is about 760 nC cm^{-2}. This is somewhat smaller than that of **A10**, but has slower relaxation to the antiferroelectric state, so it contributes to the dielectric constant in a wider range than as seen for **A10**.

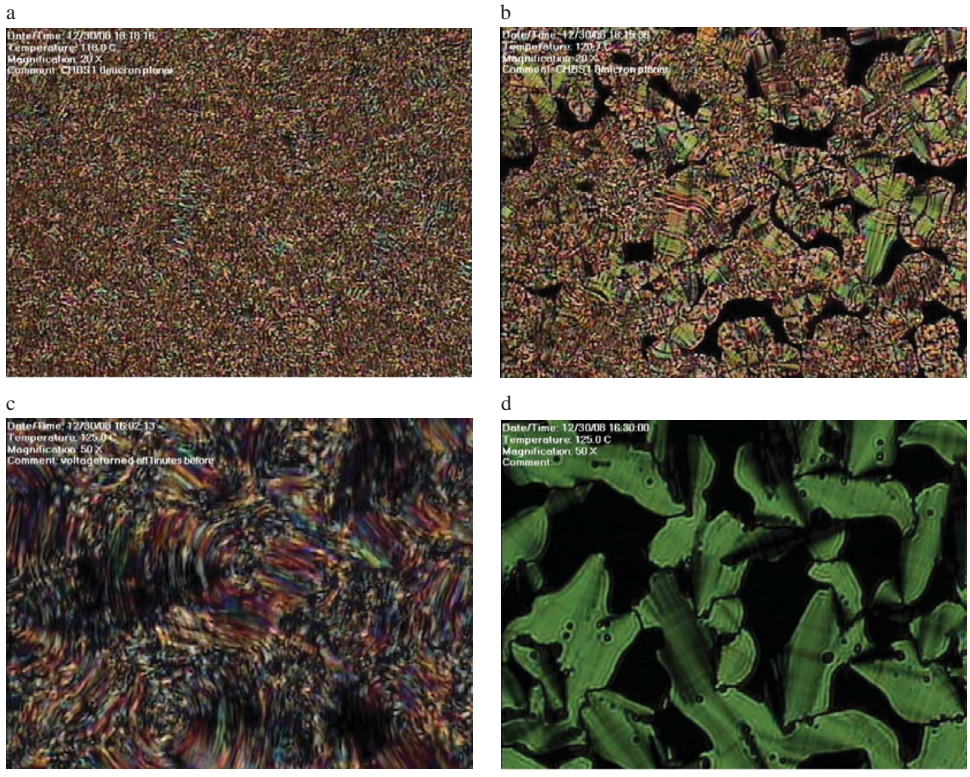

Figure 4. Textures of an 8 μm film with planar alignment of **A10** in the crystalline phase at 118°C (a), in the mesophase without any voltage treatment before at 122°C (b), in the mesophase after a 5 V μm^{-1} field is applied for 10 s and turned off (c), and when a 5 V μm^{-1} field is applied at 23 Hz (d). The pictures represent 0.4 mm x 0.3 mm areas.

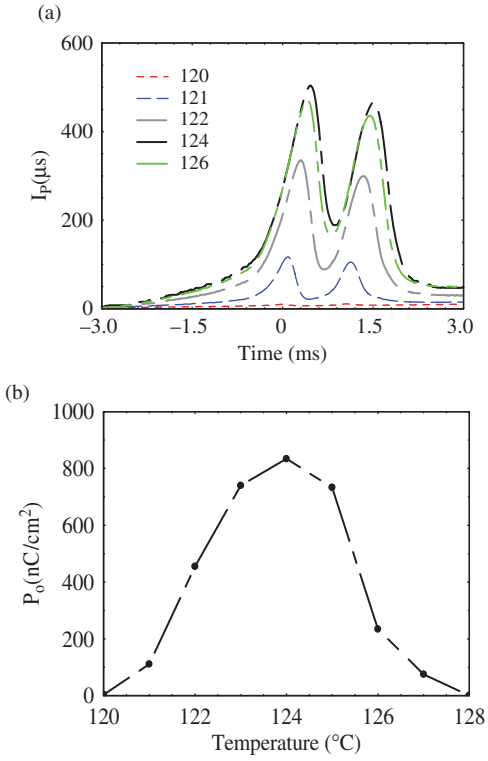

Figure 5. (a) Time dependence of the polarisation current at different temperatures of **A10** in °C; (b) Temperature dependence of the polarisation of **A10** measured by a triangular field method (colour version online).

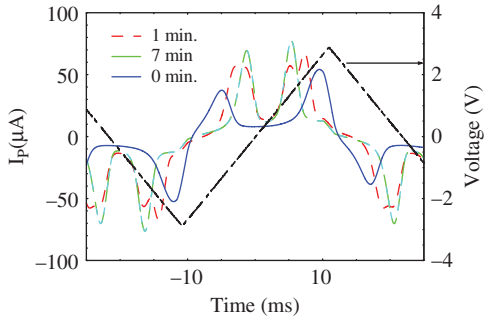

Figure 6. Variation of the polarisation current of **A10** in time while a 12 V μm^{-1} triangular wave form electric field was applied (colour version online).

4. Results and discussion

The results of this work are summarised in Tables 1 and 2. From the tables, we can see that when the terminal alkyl chains of compounds **A*n*** become longer, better mesomorphic properties are obtained. At the same time, larger spontaneous polarisation (from $P = 130$ nC cm^{-2} to $P \sim 850$ nC cm^{-2}) is observed. It is difficult to explain this fact. To our knowledge, there is no precedent about the striking increase of P which originates from the extension of the external aliphatic chain.

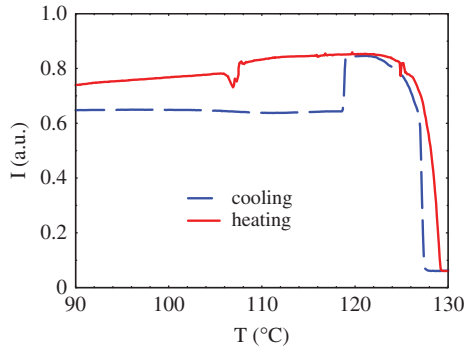

Figure 7. Temperature dependence of the transmitted light intensity of **A12** for cooling and heating (1°C/min) (colour version online).

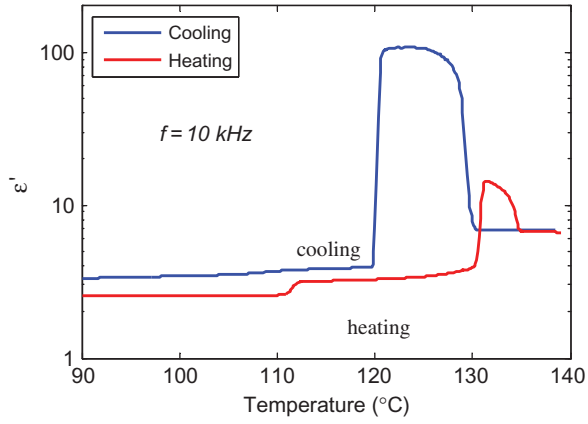

Figure 8. Temperature dependence of the dielectric constant of **A12** measured at 10 kHz (colour version online).

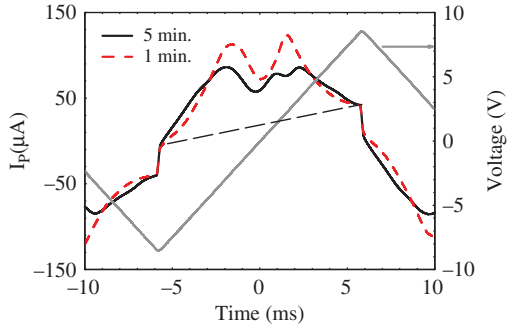

Figure 9. Time dependence of the polarisation current of **A12**, 1 min and 5 min after the triangular field is applied (colour version online).

Goodby and colleagues [20, 21] have systematically studied the effect of the molecular structure of ferroelectric liquid crystals on the magnitude of the spontaneous polarisation. They found that, although the number and type of polar groups within the

Table 1. Transition temperatures (°C) of compounds **A*n*** [16].

n	Phase transitions
4	Cr 140 Iso 130 SmX 124 Recr
8	Cr 129 Iso 125 $SmCP_A$ 123 Recr
10	Cr 130 Iso127 $SmCP_A$ 119 Recr
12	Cr 129 Iso 127 $SmCP_A$ 120 Recr

Table 2. Spontaneous polarisation (P) of compounds **A*n***.

n	P(nC·cm^{-2})
4	——
8	130
10	850
12	760

mesogen core changed, the resultant polarisations did not change appreciably. The lack of diversity in the spontaneous polarisation is probably due to the rapid orientation motion of the molecules along their long axis. Consequently, the large dipoles associated with electronegative atoms, such as oxygen and nitrogen in the functional groups of the core, have essentially isotropic properties along the long axis of the molecule. Therefore, these strong polar groups do not necessarily contribute greatly to the polarisation. The polarisation is determined by some other factors, such as the molecular size, density changes, the magnitude of the tilt angle, and differences in the interactions between the chiral centre and polar groups on the same molecule or with neighbouring molecules.

Goodby *et al.* summarised their investigation for the effect of rotational freedom of the chiral centre on the magnitude of the spontaneous polarisation. Trapment of the motion of the chiral centre relative to the long axis of the molecule can have extraordinary effects on the magnitude of the polarisation. The nature and environment of the chiral centre play a major role in determining the ferroelectric properties of liquid crystalline materials.

There are a number of forms of trapment of the chiral centre. Some investigated examples of trapment can be listed as follows:

(a) trapping by the core;
(b) damping by extension of the external aliphatic chain;
(c) trapment by branching;
(d) trapment by reducing the flexibility in the terminal chiral chain.

On the trapment of the motion of the dipole by damping, Goodby *et al.* [22] have explained the mechanism as follows:

"In the situation where the external chain is short, the chiral center is expected to be rotating relatively freely with respect to the rest of the molecule. When the external chain is extended, the chiral center and a certain portion of the aliphatic chain are supposed to spend more time lying along the long axis of the molecule. As the chiral cent has a fixed spatial arrangement with respect to its local environment, it is expected to spend more time in an orientation where the smaller groups attached to the chiral atom are in an off-axis position. This in turn will fix the orientation of the dipole at the chiral center."

The above discussion on damping by extension of the external aliphatic chain for chiral ferroelectric liquid crystals can explain the increase of P with terminal chain extension in bent-core liquid crystals **A*n***. Although the bent-core liquid crystals are achiral molecules, since 2,3-difluoro substituents are introduced into the terminal phenyl groups of tolane, the bent portion causes intramolecular steric hindrance which can also lead to intermolecular rotational interference as chiral molecules. Otherwise, when 2,3-difluoro substituents are introduced into the terminal phenyl groups of tolane, a very strong dipole forms which becomes the origin of the spontaneous polarisation in these bent-core liquid crystals. With extension of the external aliphatic chain, the mesophases become more stable, and the arrangement of the ordered molecules becomes more orderly. As the intermolecular interactions increase, the freedom of rotational movement of the dipole of C–F is damped, which will fix the orientation of the dipole. Because the fluorine atom is the largest electronegative atom, the dipole which is composed of two C–F bonds is very strong. Although the increase of the length of the terminal alkyl chain leads to a slightly larger intermolecular interaction, the magnitude of P shows a striking increase.

In conclusion, interesting mesomorphic properties were observed in the bent-core liquid crystals.

References

[1] Etxebarriaa, J.; Ros, M.B. *J. Mater. Chem.* **2008**, *18*, 2919–2926.
[2] Pelzl, G.; Weissflog, W. Mesophase Behaviour at the Borderline Between Calamitic and "Banana-shaped" Mesogens. In *Thermotropic Liquid Crystals-Recent Advances*; Ramamoorthy, A., Ed.; Springer: Dordrecht, 2007; Chapter 1.
[3] Jákli, A.; Bailey, C.; Harden, J. Physical Properties of Banana Liquid Crystals. In *Thermotropic Liquid Crystals-Recent Advances*; Ramamoorthy, A., Ed.; Springer: Dordrecht, 2007; Chapter 2.
[4] Hough, L.E.; Spannuth, M.; Nakata, M.; Coleman, D.A.; Jones, C.D.; Dantlgraber, G.; Tschierske,

C.; Watanabe, J.; Körblova, E.; Walba, D.M.; Maclennan, J.E.; Glaser, M.A.; Clark, N.A. *Science* **2009**, 452–456.
[5] Link, D.R.; Natale, G.; Shao, R.; Maclennan, J.E.; Clark, N.A.; Körblova, E.; Walba, D.M. *Science* **1997**, *278*, 1924–1927.
[6] Harden, J.; Mbanga, B.; Éber, N.; Fodor-Csorba, K.; Sprunt, S.; Gleeson, J.T.; Jákli, A. *Phys. Rev. Lett*. **2006**, *97*, 157802–157809.
[7] Jákli, A. *Liq. Cryst. Today* **2002**, *11*, 1–5.
[8] Eichhorn, S.H.; Paraskos, A.J.; Kishikawa, K.; Swager, T.M. *J. Am. Chem. Soc*. **2002**, *124*, 12742–12751.
[9] Yelamaggad, C.V.; Nagamani, S.A.; Nair, G.G.; Rao, D.S.S.; Prasad, S.K.; Jákli, A. *Liq. Cryst*. **2002**, *29*, 1181–1185.
[10] Dantlgraber, G.; Shen, D.; Diele, S.; Tschierske, C. *Chem. Mater*. **2002**, *14*, 1149–1158.
[11] Reddy, R.A.; Tschierske, C. *J. Mater. Chem*. **2006**, *16*, 907–961.
[12] Guo, Y.M.; Li, B.Z.; Yang, Y.G.; Wen, J.X. *Mol. Cryst. Liq. Cryst*. **2008**, *493*, 57–64.
[13] Yelamaggad, C.V.; Mathews, M.; Nagamani, S.A.; Rao, D.S.S.; Prasad, S.K.; Findeisen, S.; Weissflog, W. *J. Mater. Chem*. **2007**, *17*, 284–298.
[14] Yang, Y.G.; Li, H.F.; Wang, K.; Wen, J.X. *Liq. Cryst.* **2001**, *28*, 375–379.
[15] Wang, K.; Li, H.F.; Wen, J.X. *J. Fluorine. Chem*. **2001**, *109*, 205–208.
[16] Wang, K.; Jákli, A.; Li, H.F.; Yang, Y.G.; Wen, J.X. *Liq. Cryst*. **2001**, *28*, 1705–1708.
[17] Jákli, A.; Saupe, A. *One- and Two-dimensional Fluids*; Taylor & Francis: New York, 2006.
[18] Lagerwall, S.T. *Ferroelectric and Antiferroelectric Liquid Crystals*; Wiley-VCH: Wilheim, 1999.
[19] Jákli, A.; Nair, G.G.; Lee, C.K.; Chien, L.C. *Liq. Cryst*. **2001**, *28*, 489–494.
[20] Chin, E.; Goodby, J.W.; Geary, J.M.; Patel, J.S.; Leslie, T.M. *Mol. Cryst. Liq. Cryst*. **1987**, *146*, 325–339.
[21] Patel, J.S.; Goodby, J.W. *Opt. Eng*. **1987**, *26*, 23–384.
[22] Goodby, J.W.; Patel, J.S.; Chin, E. *J. Phys. Chem. Lett*. **1987**, *91*, 5151–5152.